International Journal of Power and Energy Systems, Vol. 42, No. 10, 2022
An Open Access Paper

OPTIMAL SWITCHING LOSS REDUCTION IN THREE-PHASE VSI USING THRESHOLDED RIDER OPTIMIZATION ALGORITHM

G. Rajeshkumar* and P. Sujatha Therese**

Abstract

This paper intends to develop a variable switching frequency system for switching loss minimization in a three-phase voltage source inverter. Switching losses are associated with the present value in switching instants, device voltage, and the number of commutations. Here, the number of commutations is minimized by varying the switching frequency over the fundamental period. The reduced switching loss is attained by optimizing the modulation index (MI) and reference angle. Thus, optimal switching patterns are generated with the optimized constraints, where the average value of switching losses over an entire period is determined, which has to be reduced. Accordingly, here, the optimization of MI and reference angle is carried out by thresholded rider optimization algorithm, which is the modification of the rider optimization algorithm. Finally, the experimental analysis is carried out for MI and a reference angle with respect to the switching loss parameter and total harmonic distortion.

Key Words

Voltage source inverter, switching losses, modulation index, reference angle, threshold basis

1. Introduction

Numerous scientific centres still carry out analysis that intends to develop this effectiveness. Initially, this issue is substantial in three-phase voltage source inverter (VSI) [1]–[3] that often functions with comparatively increased frequencies. This problem moreover focuses on direct current–direct current converters; on the other hand, their appliance is much lesser than the usage of VSIs [4]–[8]. Power losses in VSI take place mostly in semiconductor components, first in insulated-gate bipolar transistor (IGBTs) and in their unrestrictive diodes [9]. The entire loss of power in semiconductor components is a sum of the switching losses and conduction losses [10]–[15]. Nevertheless, there was no impact due to these losses as their minimization needs a reduction of the collector emitter voltage all through the conduction process [16]–[18]. The switching losses take place throughout both the transistor turn-off and turn-on process and it is based on the subsequent constraints: the load current, dynamic constraints of the specified IGBT, and voltage distributed to three-phase VSI [19]–[24]. This constraint is based on resistance and changing degrees in the gate-driver circuit [25]–[28]. The switching losses could be minimized by the exploitation of soft switching schemes [29]–[33]. It has considerable meaning while inverters function with pulse width modulation [34]–[37]. The major contribution of this paper is depicted in the following.

This paper intends to present a new variable switching frequency system for switching loss minimization in a three-phase VSI. In the presented work, the number of commutations is reduced by altering the switching frequency over the fundamental period. The minimal switching loss is attained by optimizing the MI and reference angle. Here, optimal switching patterns are produced with the optimized constraints, in which the average switching losses over an entire period are identified, which have to be minimized. For attaining optimal MI and reference angle, this work introduces a new thresholded rider optimization algorithm (T-ROA) approach. The overall organization of the work is as follows: Section 2 portrays the literature work. Section 3 describes the representation of the basic three-phase VSI. Section 4 presents the optimal tuning of switching frequency by improved rider optimization algorithm (ROA). Section 5 discusses experimental outcomes, and Section 6 concludes the paper.

2. Representation of Basic Three-Phase VSI

2.1 Proposed Methodology

The overall diagrammatic representation of the proposed model is shown in Fig. 1. In this research work, a novel approach has been introduced for attaining the reduced switching loss in a three-phase VSI. In such systems, the

* Kudankulam Nuclear Power Project, Kudankulam, Radhapuram, Tamil Nadu, India; e-mail: kumargrajesh96@gmail.com
** Noorul Islam University, Thuckalay, Kumaracoil, India
Corresponding author: G. Rajeshkumar
Recommended by Prof. Khaled El-Naggar
(DOI: 10.2316/J.2022.203-0191)

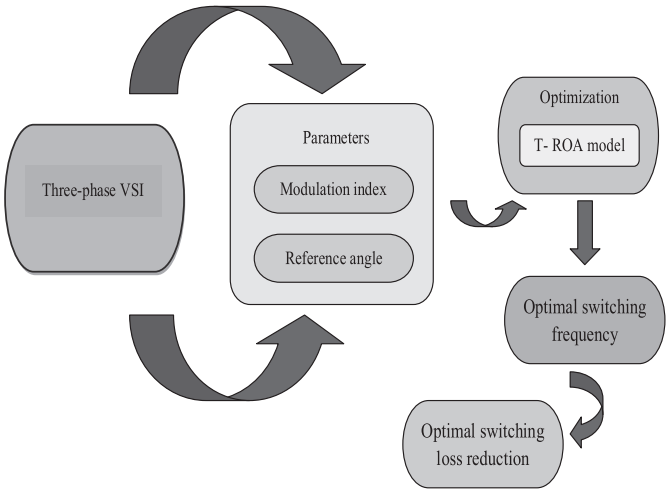

Figure 1. Overall representation of the adopted model.

switching losses are associated with the present value in switching interval, count of commutations, and device voltage. For an efficient system, the counts of commutations have to be reduced, which is attained by varying the switching frequency over the fundamental period. Accordingly, the constraints, namely MI and reference angle, have to be tuned such that reduced switching loss could be attained. Here, the MI and reference angle are subjected to optimization using modified ROA, called T-ROA, by which optimal pulses are generated, where the average value of switching losses over an entire period is discovered that has to be reduced. The main objective function of this research work intends to minimize the switching loss by optimal tuning of the optimal switching frequency.

3. Optimal Tuning of Switching Frequency by Improved Rider Optimization Algorithm

3.1 Optimizing the Switching Frequency

Switching losses are associated with the current value, count of commutations, and device voltage in switching intervals. Switching voltage is inflicted by the direct current link (V_{DC}) and the current at the output is fixed as sinusoidal signal ($i_a(t) = \hat{I}\cos(\omega t + \phi)$) for supplying a three-phase load. Here, the count of commutations was minimized by varying the switching frequency f_{sw} with respect to the fundamental period, thus promoting the variable switching frequency (VSF) technique. The switching loss for every reference angle θ is given in (7), where M denotes the switching transition times, and $\hat{I}$ specifies the sinusoidal peak value of current.

$$P_{\mathrm{loss}}(\theta) = M.V_{\mathrm{DC}}..\hat{I}.\ |\cos(\theta - \phi)|\,. \tag{1}$$

The average switching loss for an entire period is given in (2), where ϕ indicates the load angle, θ denotes the reference angle, $P_{\mathrm{loss}}(\theta)$ signifies the switching loss for every reference angle, m indicates the modulation index (MI), 2π specifies the period, and the value of 2 denotes the count of commutations for every switching intervals.

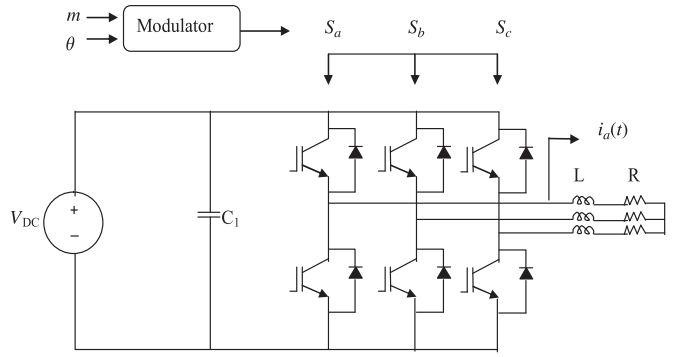

Figure 2. Representation of source, modulation system, inverter, and load.

$$P_{\mathrm{avg,\ loss}} = \frac{2}{2\pi}\int_0^{2\pi} P_{\mathrm{loss}}(\theta).f_{\mathrm{sw}}(m,\,\theta,\,\varphi).d\theta. \tag{2}$$

The reduction of $P_{\mathrm{avg,\ loss}}$ is considered as the target of the optimization. During the optimization process, the entire constants, namely, current peak value and bus voltage, are avoided as they are found inappropriate for the optimization results. It is given in (3).

$$H^*(f_{\mathrm{sw}}(m,\,\theta,\,\varphi)) = \int_0^{2\pi} |\cos(\theta - \varphi)|.f_{\mathrm{sw}}(m,\,\theta,\,\varphi).d\theta. \tag{3}$$

When there is a variation in switching frequency, there will be a trade-off among the root mean square (rms) value of output current ripple, denoted by i_{rms} and the count of commutations. That is, the optimal pattern of switching frequency has to follow a similar I_{rms} value as constant switching frequency (CSF).

Accordingly, $f_{\mathrm{sw}}(m,\,\theta,\,\phi)$ is computed based on (4), where M_f is attained from a look up table (LUT) based on m, θ, ϕ. The data of LUT are computed for every condition with the optimization process. Furthermore, M_f is multiplied with the CSF, $f_{\mathrm{sw,\ constant}}$ for attaining the actual f_{sw}. For every load angle (ϕ_{load}), the frequency patterns will be loaded owing to static load analysis. With M_f, every CSF could be updated into VSF that is optimal for loss minimization in switches. M_f is much influenced by the deviations in m; however, it was insensitive to deviations in ϕ. Thus, the symmetry of deviation over θ is noticeable. The diagrammatic representation of the VSI system is given in Fig. 2.

$$f_{\mathrm{sw}}(m,\,\theta,\,\varphi) = M_f * f_{\mathrm{sw,\ constant}}. \tag{4}$$

3.2 Objective Model

The objective function of the proposed research work is to attain the optimal switching frequency as given in (5), in which Ro indicates the objective function, C denotes the optimal rms value to attain. Here, C is attained by I_{rms} per unit with the MI function and with the CSF of space vector pulse width modulation (SVPWM) for the entire period.

$$Ro = \mathrm{Min}\ [H^*(f_{\mathrm{sw}}(m,\,\theta,\,\varphi)) + [i_{\mathrm{rms}} - C]]\,. \tag{5}$$

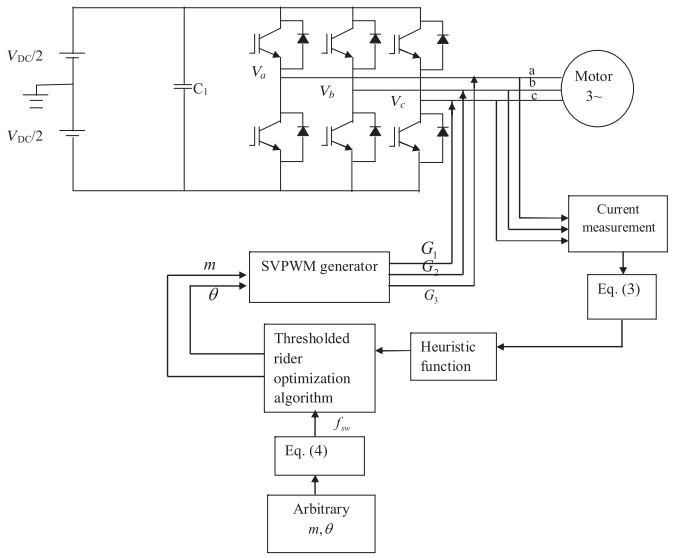

Figure 3. Proposed T-ROA model.

Figure 4. Solution encoding for optimal switching frequency.

The overall interconnected diagram related to objective model, optimization algorithm, and three-phase VSI is depicted in Fig. 3. In this novel design, the optimal switching pattern is generated by a modified optimization algorithm called T-ROA. Here, the MI m and reference angle θ are given as input for solution encoding, which has to be tuned optimally. Here, m and θ should be tuned such that the switching frequency should be optimal for attaining reduction in switching losses. The solution encoding process is given in Fig. 4.

3.3 Rider Optimization Algorithm

The parameters m and θ are subjected to optimization using T-ROA model. In general, ROA [25] is dependent on the cluster of riders, moving towards a similar destination to be the champion of the race. The amazing idea concerning ROA is its performance with reduced optimization time, thus performing better than the other artificial computing and nature-inspired optimizations.

The rider's position is initialized as given in (6), in which Y and U indicate the count of total coordinates and riders. $Z^{\tau}(g,h)$ indicates the position of p^{th} rider at τ. A total of B, F, G, and A riders, such as bypass, followers, overtakers, and attackers, are considered in this work.

$$Z^{\tau} = \{Z^{\tau}(g,\, h)\}\,;(1 \le g \le U)\,;(1 \le h \le Y)\,. \quad (6)$$

Assume that the angles related to the position, steering, and coordinate of the vehicle of the g^{th} rider is θ_g, $N^{\tau}_{g,h}$, and δ. In addition to the constraints of the vehicle, namely, brake, gear, and accelerator of g^{th}, the riders are represented as r_g, Q_g, and a_g, correspondingly. The gear Q_g attains a value between 0 and 4, whereas the brake values r_g and accelerator a_g lie between 0 and 1.

The leading rider is predetermined by success rate or the riders obtaining the higher success rate are said to be a leader. According to the standard ROA model, there are four kinds of riders: bypass rider bypasses the foremost path to arrive at the destination, follower tempts to follow the leader, overtaker concerns his own path for arriving at the target, and attacker arrives at the destination by holding the rider's position. Every rider follows a predefined policy to arrive at the target through the effectual management of the steering, gear, brake, and accelerator of the vehicle. The rider's position is varied by tuning these constraints following a predetermined approach and the procedure is performed till the off-time, τ_{off}. The bypass rider does not follow the leader as the general path is bypassed that is arithmetically formulated as given in (7), which is the standard equation of the bypass rider in the ROA.

$$Z^{\tau+1}_{g,h}\ (B) = \beta\ \left[Z^{\tau}_{\gamma,\,h} * \alpha\ (h)\ +\ Z^{\tau}_{\eta,\,h} * (1 - \alpha\ (h))\right], \quad (7)$$

where β indicates an arbitrary number attaining the values between 0 and 1, γ denotes the arbitrary number acquiring the values between 1 and U, and η refer to the arbitrary number lying between 1 and U. Simultaneously, α portrays the arbitrary number considering the value between 0 and 1 of size $(1 \times Y)$. Therefore, the position of the rider is updated at the termination of the individual's iteration to confirm the champion. Concurrently, the follower's position is updated depending on the leader to arrive at the target that is designed as shown in (8). Here, b denotes the coordinate selector, leaders' position be Z^{L}, L indicates the index of the leader, $Z^{L}(L,\, b)$, $N^{\tau}_{g,b}$ refers to the steering angle of g^{th} rider in b^{th} coordinate, and ∂^{τ}_{g} indicates the distance covered by g^{th} rider.

$$Z^{\tau+1}_{g,\,h}\ (F) = Z^{L}\,(L,\, b) + \left[\cos\left(N^{\tau}_{g,\,b}\right)\ * Z^{L}\,(L,\, b) * \partial^{\tau}_{g}\right]. \quad (8)$$

Here, the distance enclosed by the rider is approximated by multiplying τ_{off} and velocity. The overtaker's position will be based on the direction indicator, success rate, and coordinate selector, and the corresponding update is specified in (9). Here, $Z^{\tau}_{g,\,b}$ denotes the position of g^{th} rider in b^{th} coordinate and I^{τ}_{g} indicates the directional indicator of g^{th} rider in τ and it is computed based on the success rate as given in (10).

$$Z^{\tau+1}_{g,\,b}\ (O) = Z^{\tau}_{g,\,b} + \left[I^{\tau}_{g} * Z^{L}\ (L,\, b)\right], \quad (9)$$

$$I^{\tau}_{g} = \left[\frac{2}{1 - \log\ (F_g)}\right] - 1, \quad (10)$$

where F_g portrays the success rate of g^{th} rider at τ and the higher success rate is observed among U riders, whose value lies between 0 and 1. The evaluation of coordinate selector is dependent on the variation in the positions of the leading rider and g^{th} rider. Alternatively, the attacker attempts to arrive at the target following the leader with the position update identical to that of the follower. The attacker's position is given in (11).

$$Z_{g,h}^{\tau+1}(A) = Z^{L}(L, b) + \left[\cos\left(N_{g,b}^{\tau}\right) * Z^{L}(L, b) + \partial_{g}^{\tau}\right]. \quad (11)$$

The rider constraints are updated at the termination of the iteration to find out the desired solution. Therefore, the constraints to be updated consist of the accelerator, gear, ride off-time, brake, and steering angle together with the activity counter (includes 0 or 1 depending on success rate), which is updated at the termination of the iteration. The phases of optimization are continued until the termination. Finally, the optimal solution is attained by the optimization approach.

3.4 Proposed T-ROA Algorithm

In the proposed model, the update of bypass rider, follower, attacker, and overtaker takes place based on the threshold value as shown in (12). Accordingly, if the fitness of the current solution, fit, is improved than previous fitness, fit^{pr} and if the random variable, ra, is greater than threshold, Th based on (12), the bypass rider gets updated; otherwise, the follower gets updated. On the contrary, if the fitness, fit, is not improved than previous fitness, fit^{pr} and if the random variable, ra, is greater than the threshold, Th, the overtaker rider gets updated; otherwise, the attacker gets updated. As the modification of the proposed optimization is based on threshold, the adopted model is named as T-ROA. In (12), fit specifies the fitness value of the current solution, and fit_n denotes the fitness value of the entire solutions. The pseudocode of presented T-ROA is highlighted in Algorithm 1.

$$\mathrm{Th} = (0.9 * \mathrm{fit}/\max(\mathrm{fit}_n)) + 0.1. \quad (12)$$

Algorithm 1: Proposed T-ROA Model

```
Input: Random positions of riders, Z^τ_{g,b}
Output: Leading rider, Z^L
  Assign the population
  Assign the rider constraints
  Determine the success rate
  While τ < τ_off
    for g = 1 to U
      If fit is improved than fit^pr
        if ra > Th
          Update bypass position rider as per (7)
        else
          Update follower position as per (8)
      If fit is not improved than fit^pr
        if ra > Th
          Update overtaker position as per (9)
        else
          Update attacker position as per (11)
      Rank riders depending on success rate
      Choose rider with higher success rate
      as leading one.
      Update the rider constraints
      Return Z^L
      τ = τ + 1
    end for
  end while
End
```

4. Results and Discussions

4.1 Simulation Procedure

The presented T-ROA-based optimal switching frequency in VSI systems was simulated in MATLAB, and the experimental analysis was carried out. Here, when the ϕ of load 5, $\phi_{\mathrm{load5}} = -35^0$, the resistance of load 5, R_{load5} will be 5Ω. Similarly, when the ϕ of load 10, $\phi_{\mathrm{load10}} = -20^0$, the resistance of load 10, R_{load10} will be 10Ω. Also, when the ϕ of load 15, $\phi_{\mathrm{load15}} = -13^0$, the resistance of load 15, R_{load15} will be 15Ω and when the ϕ of load 20, $\phi_{\mathrm{load20}} = -8^0$, the resistance of load 20, R_{load20} will be 20Ω. In the next implementation, the presented model was compared over conventional models namely, genetic algorithm (GA) [26], particle swarm pptimization (PSO) [27], firefly (FF) [28], grey wolf optimization (GWO) [29] and ROA [25], and the analysis was carried out for determining the switching loss parameter, E_{sw} with respect to m and θ.

4.2 Effect on Modulation Index

The presented analysis on switching loss parameter using T-ROA for varied loads with respect to m is described in this section. From Fig. 5(a), when $\phi_{\mathrm{load20}} = -8^0$, the adopted model for $m = 0.1$ is 19.59% better than PSO, 18.37% better than GWO, and 18.37% better than ROA schemes. In the same way, from Fig. 5(d), when $\phi_{\mathrm{load5}} = -35^0$, the suggested T-ROA scheme for $m = 0.25$ is 33.33% superior to PSO, 15.56% superior to FF, and 8.89% superior to GWO schemes. Thus, the enhancement of the adopted model in terms of E_{sw} has been validated in a better way.

4.3 Effect on Reference Angle

The analysis on E_{sw} with respect to θ using T-ROA for different loading conditions is portrayed by Fig. 6. From Fig. 6(a), at $\phi_{\mathrm{load20}} = -8^0$, when $\theta = 0.79$, the suggested T-ROA model is 26.42% superior to GA, 24.53% superior to PSO, 24.53% superior to FF, 1.9% superior to GWO, and 5.66% superior to ROA schemes. Therefore, it is confirmed that adopted T-ROA offers better E_{sw} when evaluated with the other traditional schemes.

4.4 Total Harmonic Distortion (THD) Analysis

The THD analysis of the presented T-ROA-based switching loss reduction in a three-phase VSI over the conventional algorithms is portrayed in Table 1. From Table 1, for load 5, the adopted scheme is 56.41% better than GA, 74.81% better than PSO, 45.78% better than FF, 49.86% better than GWO, and 51.29% better than ROA schemes. Hence, the superiority of the presented T-ROA approach has been confirmed from the simulation results on harmonic distortion minimization.

4.5 Convergence Analysis

The convergence analysis of the presented T-ROA model for optimal switching loss reduction is given in Fig. 7. From

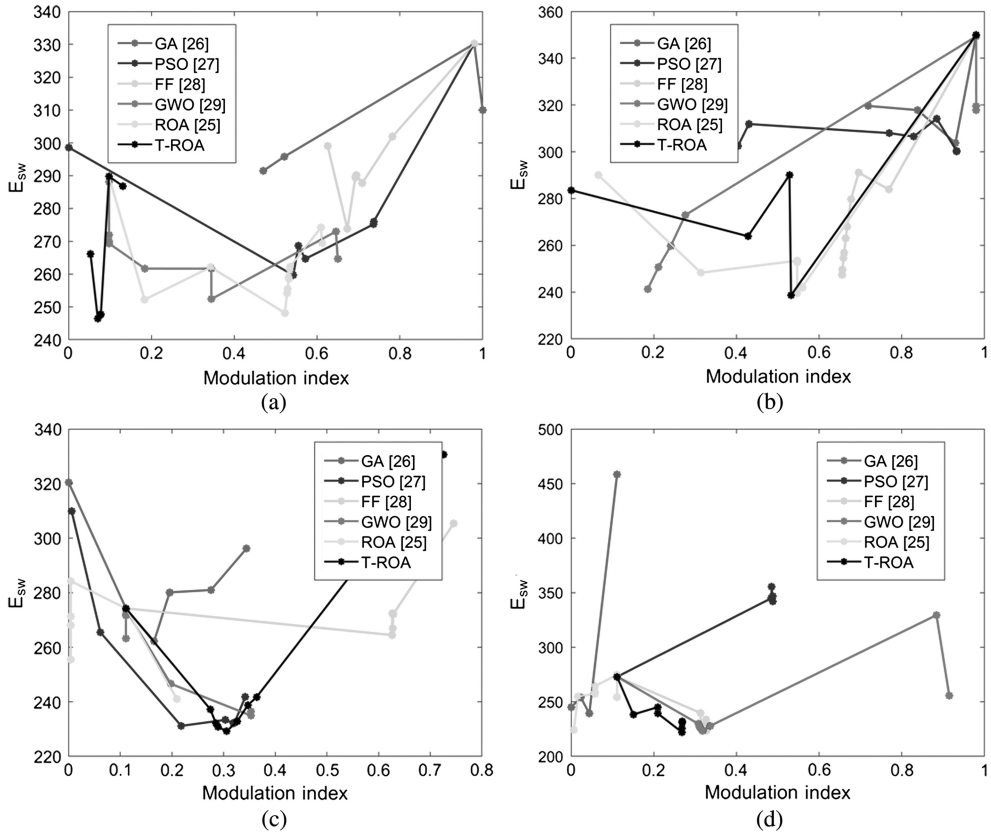

Figure 5. Analysis on switching loss parameter with respect to MI for the proposed and conventional models for (a) $\phi_{\text{load20}} = -8^0$; (b) $\phi_{\text{load15}} = -13^0$; (c) $\phi_{\text{load10}} = -20^0$; (d) $\phi_{\text{load5}} = -35^0$.

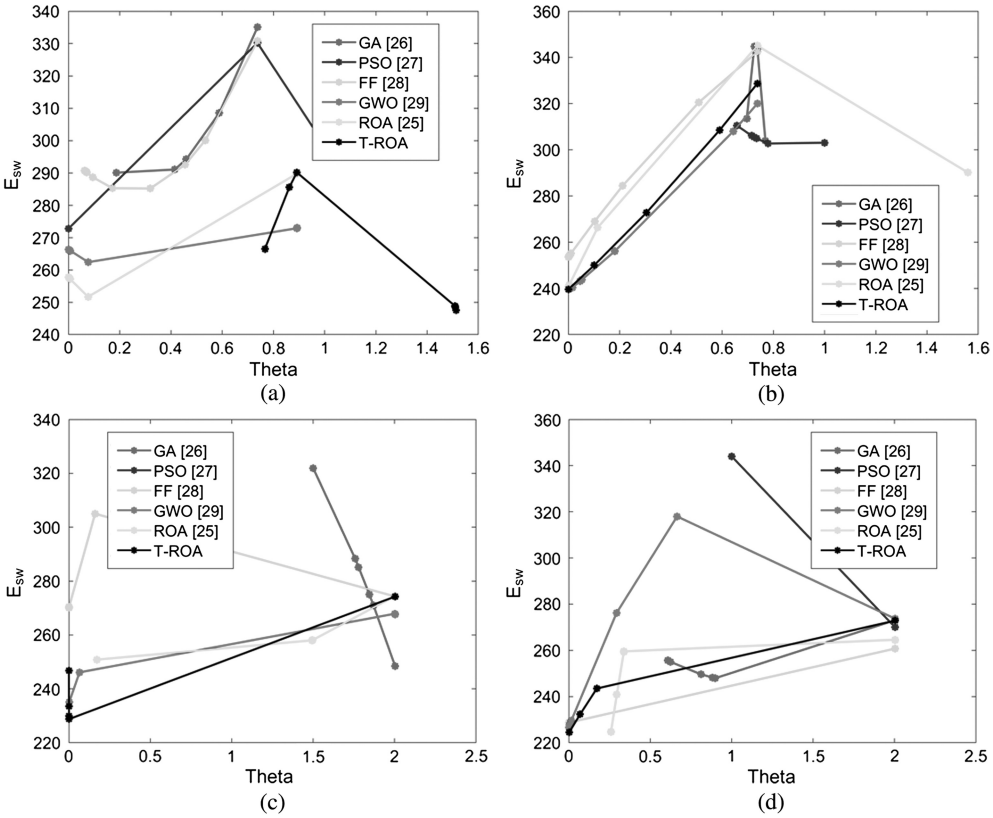

Figure 6. Analysis on switching loss parameter with respect to reference angle for the proposed and conventional models for (a) $\phi_{\text{load20}} = -8^0$; (b) $\varphi_{\text{load15}} = -13^0$; (c) $\varphi_{\text{load10}} = -20^0$; (d) $\varphi_{\text{load5}} = -35^0$.

Table 1
THD Analysis of the Proposed and Conventional Models

	GA [26] (db)	PSO [27] (db)	FF [28] (db)	GWO [29] (db)	ROA [25] (db)	Base-Case (db)	T-ROA (db)
Load 5	−6.48	−3.75	−8.07	−7.46	−7.25	−11.58	−14.8
Load 10	−3.22	−8.24	−3.09	−12.517	−3.99	−8.99	−14.68
Load 15	−13.18	−4.85	−4.776	−4.024	−6.34	−5.95	−13.60
Load 20	−13.25	−12.10	−6.42	−16.51	−11.49	−5.99	−20.19

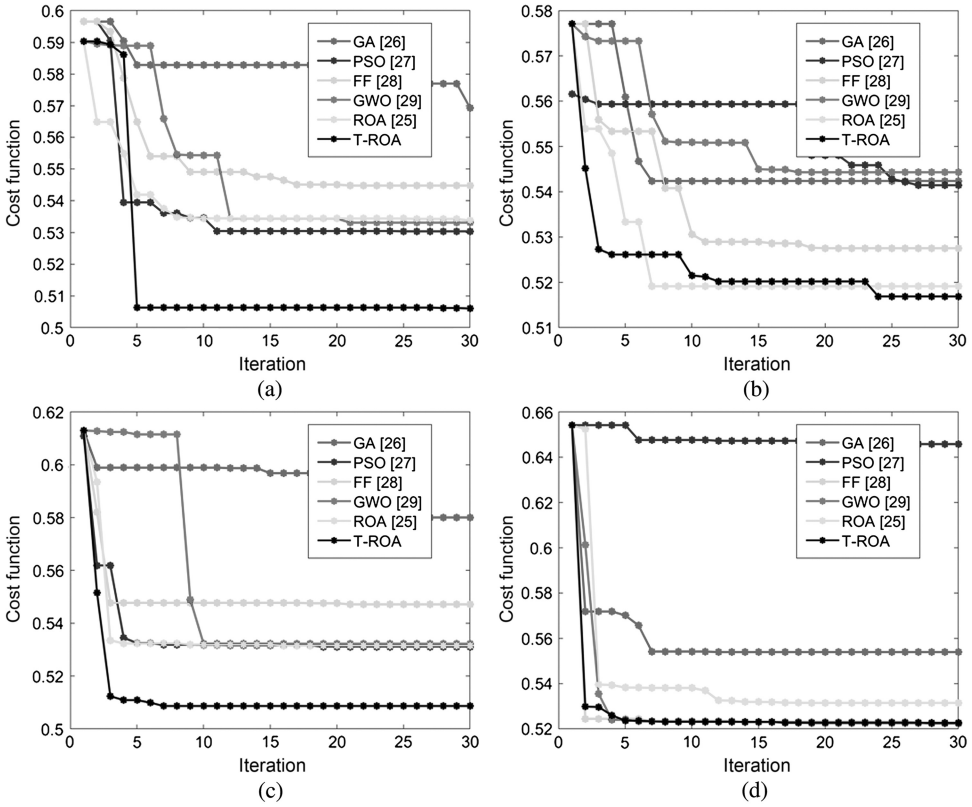

Figure 7. Convergence analysis of the proposed and conventional models: (a) $\varphi_{\text{load20}} = -8^0$; (b) $\varphi_{\text{load15}} = -13^0$; (c) $\varphi_{\text{load10}} = -20^0$; (d) $\varphi_{\text{load5}} = -35^0$.

Fig. 7(a), at 30th iteration, the cost function of the adopted scheme for $\phi_{\text{load20}} = -8^0$ is 11.98% better than GA, 4.13% better than PSO, 7.07% better than FF, 5.1% better than GWO, and 5.1% better than ROA models. Finally, from Fig. 7(d), the introduced model at 30th iteration for $\phi_{\text{load5}} = -35^0$ is 6.89% superior to GA, 23.56% superior to PSO, and 1.53% superior to ROA schemes. Thus, the betterment of the suggested T-ROA model was proved in terms of the cost analysis.

5. Conclusion

This paper has presented a variable switching frequency system for switching loss reduction in a three-phase VSI. To attain the optimal MI and reference angle, this work has introduced a new T-ROA approach. The performance of the adopted method T-ROA was compared over other traditional schemes to validate the effectiveness of the adopted method. From the analysis, when $\phi_{\text{load1}} = -35^0$, the adopted model for $m = 0.25$ was 33.33% superior to PSO, 15.56% superior to FF, and 8.89% superior to GWO schemes. Thus, the performance of the proposed T-ROA-based optimal switching loss reduction in a three-phase VSI was proved to be efficient than other conventional models.

References

[1] W. Chen, H. Sun, X. Gu, and C. Xia, Synchronized space-vector PWM for three-level VSI with lower harmonic distortion and switching frequency, *IEEE Transactions on Power Electronics*, *31*(9), 2016, 6428–6441.

[2] O. Oñederra, I. Kortabarria, I.M. de Alegría, J. Andreu, and J.I. Gárate, Three-phase VSI optimal switching loss reduction using variable switching frequency, *IEEE Transactions on Power Electronics*, *32*(8), 2017, 6570–6576.

[3] F. Mwasilu, E. Kim, M.S. Rafaq, and J. Jung, Finite-set model predictive control scheme with an optimal switching voltage vector technique for high-performance IPMSM drive applications, *IEEE Transactions on Industrial Informatics*, *14*(9), 2018, 3840–3848.

[4] T.N. Nguyen, A. Luo, and M. Li, A simple and robust method for designing a multi-loop controller for three-phase VSI with an LCL-filter under uncertain system parameters, *Electric Power Systems Research*, *117*, 2014, 94–103.

[5] M. Trabelsi, M. Boussak, and M. Benbouzid, Multiple criteria for high-performance real-time diagnostic of single and multiple open-switch faults in ac-motor drives: Application to IGBT-based voltage source inverter, *Electric Power Systems Research*, *144*, 2017, 136–149.

[6] S. Wang, C. Li, C. Che, and D. Xu, Direct torque control for 2L-VSI PMSM using switching instant table, *IEEE Transactions on Industrial Electronics*, *65*(12), 2018, 9410–9420.

[7] K. Chen and Y. Xie, Reducing harmonics distortion in five-phase VSI using space-vector-based optimal hybrid PWM, *IEEE Transactions on Power Electronics*, *32*(3), 2017, 2098–2113.

[8] R.B. Dhumale and S.D. Lokhande, Neural network fault diagnosis of voltage source inverter under variable load conditions at different frequencies, *Measurement*, *91*, 2016, 565–575.

[9] K. Thakre, K.B. Mohanty, and A. Chatterjee, Reduction of circuit devices in symmetrical voltage source multilevel inverter based on the series connection of basic unit cells, *Alexandria Engineering Journal*, 15 November 2018.

[10] I. Ziouani, D. Boukhetala, A.-M. Darcherif, B. Amghar, and I. El Abbassi, Hierarchical control for flexible microgrid based on three-phase voltage source inverters operated in parallel, *International Journal of Electrical Power & Energy Systems*, *95*, 2018, 188–201.

[11] S. Dowruang, P. Bumrungsri, and C. Jeraputra, Improved voltage vector sequences on model predictive control for a grid connected three phase voltage source inverter, *Procedia Computer Science*, *86*, 2016, 393–396.

[12] N. Raj, J. Mathew, G. Jagadanand, and S. George, Open-transistor fault detection and diagnosis based on current trajectory in a two-level voltage source inverter, *Procedia Technology*, *25*, 2016, 669–675.

[13] A. Shokri, H. Shareef, A. Mohamed, M. Farhoodnea, and H. Zayandehroodi, A novel controller for a voltage controlled voltage source inverter to mitigation voltage fluctuations measured at the point of common coupling, *Measurement*, *59*, 2015, 216–226.

[14] O. Duque-Perez, L.-A. Garcia-Escudero, D. Morinigo-Sotelo, P.-E. Gardel, and M. Perez-Alonso, Analysis of fault signatures for the diagnosis of induction motors fed by voltage source inverters using ANOVA and additive models, *Electric Power Systems Research*, *121*, 2015, 1–13.

[15] S.B. Naderi, M. Negnevitsky, A. Jalilian, M.T. Hagh, Efficient fault ride-through scheme for three phase voltage source inverter-interfaced distributed generation using DC link adjustable resistive type fault current limiter, *Renewable Energy*, *92*, 2016, 484–498.

[16] T. Abdelkrim, T. Benslimane, A. Borni, K. Benamrane, and N. Bouarroudj, Performance evaluation of a new control scheme of distributed two-stage PV conversion system using three levels voltage source inverter for stand-alone application, *Energy Procedia*, *119*, 2017, 270–277.

[17] A.A.A. Radwan, Y.A.-R.I. Mohamed, and E.F. El-Saadany, Assessment and performance evaluation of DC-side interactions of voltage-source inverters interfacing renewable energy systems, *Sustainable Energy, Grids and Networks*, *1*, 2015, 28–44.

[18] F. Mehazzem, A.L. Nemmour, and A. Reama, Real time implementation of backstepping-multiscalar control to induction motor fed by voltage source inverter, *International Journal of Hydrogen Energy*, *42*(28), 2017, 17965–17975.

[19] M. Fateh and R. Abdellatif, Comparative study of integral and classical backstepping controllers in IFOC of induction motor fed by voltage source inverter, *International Journal of Hydrogen Energy*, *42*(28), 2017, 17953–17964.

[20] P.-E. Vidal, S. Cailhol, and F. Rotella, Generic modeling of N-level pulse width modulation voltage source inverters and their control", *IFAC-PapersOnLine*, *50*(1), 2017, 7813–7818.

[21] J. Linares-Flores, J.F. Guerrero-Castellanos, R. Lescas-Hernndez, A. Hernndez-Mndez, and R. Vzquez-Perales, Angular speed control of an induction motor via a solar powered boost converter-voltage source inverter combination, *Energy*, *166*, 2019, 326–334.

[22] S.M. Muyeen, A. Al-Durra, and J. Tamura, Variable speed wind turbine generator system with current controlled voltage source inverter, *Energy Conversion and Management*, *52*(7), 2011, 2688–2694.

[23] S.Y.M. Mousavi, A. Jalilian, M. Savaghebi, and J.M. Guerrero, Coordinated control of multifunctional inverters for voltage support and harmonic compensation in a grid-connected microgrid, *Electric Power Systems Research*, *155*, 2018, 254–264.

[24] A. Darwish, A.S. Abdel-Khalik, A. Elserougi, S. Ahmed, and A. Massoud, Fault current contribution scenarios for grid-connected voltage source inverter-based distributed generation with an LCL filter, *Electric Power Systems Research*, *104*, 2013, 93–103.

[25] D. Binu and B.S. Kariyappa, RideNN: A new rider optimization algorithm-based neural network for fault diagnosis in analog circuits, *IEEE Transactions on Instrumentation and Measurement*, *68*(1), 2019, 2–26.

[26] J. McCall, Genetic algorithms for modelling and optimisation, *Journal of Computational and Applied Mathematics*, *184*(1), 2005, 205–222.

[27] J. Zhang and P. Xia, An improved PSO algorithm for parameter identification of nonlinear dynamic hysteretic models, *Journal of Sound and Vibration*, *389*, 2017, 153–167.

[28] I. Fister, I. Fister, X.-S. Yang, and J. Brest, A comprehensive review of firefly algorithms, *Swarm and Evolutionary Computation*, *13*, 2013, 34–46.

[29] S. Mirjalili, S.M. Mirjalili, and A. Lewis, Grey wolf optimizer, *Advances in Engineering Software*, *69*, 2014, 46–61.

[30] D. Jiang and F. Wang, A general current ripple prediction method for the multiphase voltage source converter, *IEEE Transactions on Power Electronics*, *29*(6), 2014, 2643–2648.

[31] G. Grandi, J. Loncarski, and O. Dordevic, Analytical evaluation of output current ripple amplitude in three-phase three-level inverters, *IET Power Electronics*, *7*(9), 2014, 2258–2268.

[32] A. Ibrahim and M.Z. Sujod, Variable switching frequency hybrid PWM technique for switching loss reduction in a three-phase two-level voltage source inverter, *Measurement*, *151*, 2020, 107192.

[33] I.H. Shanono, N.R.H. Abdullah, H. Daniyal, and A. Muhammad, Selective harmonic elimination (SHE) based 3-phase multilevel voltage source inverter (VSI) for standalone applications, SN Applied Sciences, *1*(12), 2019, 1670.

[34] O. Oñederra, I. Kortabarria, I.M. de Alegría, J. Andreu, and J.I. Gárate, Three-phase VSI optimal switching loss reduction using variable switching frequency, *IEEE Transactions on Power Electronics*, *32*(8), 2016, 6570–6576.

[35] G. Nalcaci and M. Ermis, Selective harmonic elimination for three-phase voltage source inverters using whale optimizer algorithm, in: *2018 5th International Conference on Electrical and Electronic Engineering (ICEEE)* (IEEE, 2018), 1–6.

[36] A. Anuchin, D. Aliamkin, M. Lashkevich, D. Shpak, A. Zharkov, and F. Briz, Minimization and redistribution of switching losses using predictive PWM strategy in a voltage source inverter, in *2018 25th International Workshop on Electric Drives: Optimization in Control of Electric Drives (IWED)* (IEEE, 2018), 1–6.

[37] A. Abdelhakim, P. Davari, F. Blaabjerg, and P. Mattavelli, Switching loss reduction in the three-phase quasi-Z-source inverters utilizing modified space vector modulation strategies, *IEEE Transactions on Power Electronics*, *33*(5), 2017, 4045–4060.

[38] I. Ziouani, D. Boukhetala, A.M. Darcherif, B. Amghar, and I. El Abbassi, Hierarchical control for flexible microgrid based on three-phase voltage source inverters operated in parallel, *International Journal of Electrical Power & Energy Systems*, *95*, 2018, 188–201.

Biographies

G. Rajeshkumar was born in Kerala, India, in 1967. He received the Diploma in Electrical Engineering from State Board of Technical Education, Kerala, India, B.E in Electrical and Electronics Engineering and M.E in Power Electronics and Drives from Anna University, Chennai, India, in 1986, 2013 and 2016 respectively. He is currently working towards the Ph.D Degree in Optimal Switching Loss Reduction in Three Phase VSI, in Noorul Islam University, Thuckalay, Tamil Nadu, India.

From 1989 onwards he is working in Nuclear Power Corporation of India LTD (Government of India Enterprise) in different sections and capacities of Plant Operation, Technical Service Section, Electrical and Instrumentation section and Presently at Centralized Tender Cell as Scientific Officer/E. His research interest includes Switching Loss Reduction in Three Phase VSI using a Nature-inspired metaheuristic algorithm.

Dr. P. Sujatha Therese is currently working as a Professor in Noorul Islam University, Thuckalay, Kumaracoil. She had published three international conferences paper and nine international journal papers. Her research interest include a control system and fuzzy controllers.